Systems of Tethered Multicopters: Modeling and Control Design *

Lorenzo Fagiano †

Abstract

A class of tethered unmanned aerial vehicles is considered, featuring a chain of multicopter drones tethered one to the other. The first drone in the chain is tethered to a ground station, while the last one serves as end effector. Differently from previous contributions in the literature, here the tethers are assumed to be elastic and to transfer traction loads only. Moreover, their length can be adjusted through controlled winches installed in the ground station and on each drone. Named systems of tethered multicopters, these devices can be used for a range of applications where both long runtime and good flexibility are required. The paper describes a model of the system, and presents a hierarchical control approach based on low-level, distributed linear controllers on each drone, and a high-level model predictive controller to coordinate the whole formation. The proposed control approach is tested through numerical simulations.

1 Introduction

In the last decade, the interest in unmanned aerial vehicles (UAVs, commonly known also as drones) for civil applications has been constantly increasing across industry, academia, research institutions, governmental bodies and the society at large. The state-of-the-art of untethered UAV technologies is quite advanced: a significant number of contributions is available regarding any technical aspect, like dynamics and control ([15]), mechanical design ([8]), sensor fusion ([13]), and energy management ([10]), to name just a few. The main disadvantage of untethered UAVs is the limited operational time that can be achieved before charging or swapping the onboard batteries. To cope with this issue, tethered UAVs have been developed in recent years. The tether can be used to feed power to the drone, reducing or completely removing the on-board energy storage. Moreover, data can be transferred through the tether as well, improving the reliability and bandwidth of communication with the ground. On the other hand, the constraint imposed by the tether clearly represents a limitation in terms of agility and versatility. Regarding the state-of-the-art of tethered UAVs, studies concerned with dynamics and control ([16, 9]), interactions with ground robots ([12]), stabilization ([11]), take-off and landing ([14]), system design and

*This is the preprint and extended version of the paper "Systems of Tethered Multicopters: Modeling and Control Design", included in the Proceedings of the 2017 IFAC World Congress, Tolouse, France, 9-14 July 2017.

†Politecnico di Milano, Dipartimento di Elettronica, Informazione e Bioingegneria, Milano, Italy (e-mail: lorenzo.fagiano@polimi.it).

prototyping ([2]) are available. Moreover, several commercial products exist as well (see e.g. [3]), all of them proposing single drones tethered to the ground (or to a moving vehicle) in a stationary or almost stationary configuration for long-term video surveillance.

The first main contribution of this paper is to introduce a new class of tethered UAVs, named here Systems of TEthered Multicopters (STEM), which ideally combine the advantages of untethered and tethered UAVs. These systems are composed of two or more drones, linked by tethers to each other and to an attachment point on the ground (ground station). The use of more than one unit yields a much larger flexibility and operational range with respect to systems with a single tethered UAV, while still retaining all the advantages provided by the tether (runtime, reliability, safety, data transmission etc.). A similar concept has been explored in the literature ([18]), considering a chain of two drones whose motion is confined on a 2-dimensional manifold and whose tethers are treated as rigid links of fixed length, able to transfer both compression and traction forces. The novelties introduced in this paper are to consider an arbitrary number of tethered drones, with six degrees of freedom each (i.e. rigid bodies in a three-dimensional space), and with flexible (elastic) tethers, able to transfer only traction forces. Moreover, the tethers can be adjusted in length, thanks to controlled winches installed onboard the drones and on the ground station, hence adding more degrees of freedom to the whole system.

STEM represent rather complex, nonlinear and constrained dynamical systems. The second main contribution of this work is a control approach for STEM, consisting of local linear controllers acting on each drone (and winch), and a supervisory centralized controller in the ground station. The local controllers are static linear state-feedback laws, whose aim is to track the position and yaw references provided by the supervisory controller. The latter is a model predictive control (MPC) law ¡,which computes the position and yaw references for all the drones by solving an optimal finite-horizon control problem in real-time in a receding horizon fashion. To limit the computational complexity and obtain a convex optimization problem, the MPC law employs a linear prediction model for each drone, where the inputs are the reference position and yaw angle, and the outputs are the actual position and yaw. Such models can be readily obtained from the closed-loop dynamics of each drone under the action of their local controllers. The use of MPC allows one to easily enforce operational constraints, e.g. on the maximum tether length and on the relative position between the drones, and to consider different possible control objectives. In this respect, we provide a general formulation of the controller, and then we focus, among the many applications in which STEM could be used, on a scenario where an external source (e.g. a human pilot) provides desired values of position and yaw angle for the last drone in the chain. The supervisory controller receives such desired values and it has to automatically adjust the position and yaw of all the units in order to track them. Overall, the proposed control approach is rather straightforward to implement, modular and effective. After describing the control design aspects, we conclude the paper by presenting numerical simulation results of a chain of three drones. Besides introducing the concept of STEM and the related modeling and control design aspects, this paper also represents a first stage in our research, aimed to realize an experimental prototype of this kind of system.

2 System description and control approach

The system under consideration is depicted in Figure 1. It consists of a series of drones (quadrotor helicopters are considered here), each one tethered to the next one. The first drone is tethered to a ground station, while the last drone is tethered only to the second last. The tethers can transfer power, data and mechanical forces (only in traction), and their mass is not negligible. Moreover, differently from previous contributions dealing with similar topologies of tethered robotic systems (see e.g. [17]) the tethers here have adjustable length. This is achieved by installing controlled winches on the ground station and on each drone in the chain (except for the last one). The winches are equipped with slip-rings to achieve transfer of power and data notwithstanding the drum rotation. As shown in Figure 1-(b), the tether reaching each drone from the previous winch is assumed to act on the center of gravity, while the onboard winch is installed on a gimbal, such that the axis of rotation of the drum is below the center of gravity.

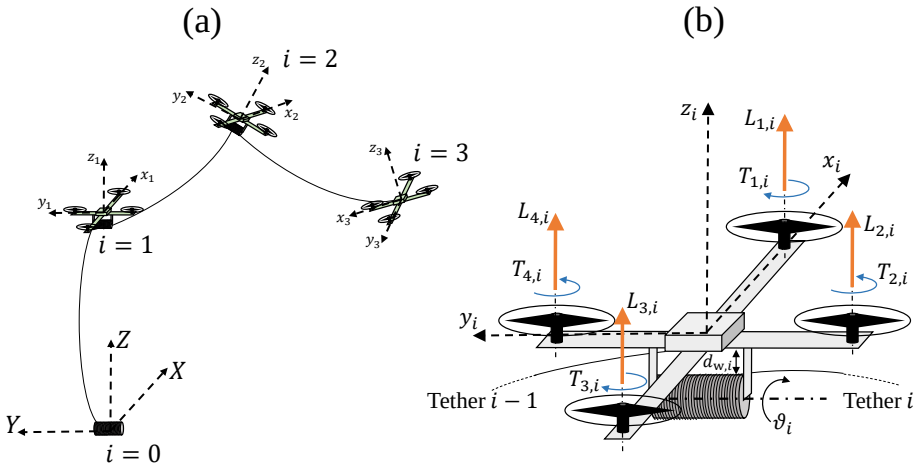

Figure 1: Sketch of the considered system: (a) chain of three tethered drones and inertial reference system G, (b) drone i with tether $i-1$ connected at the center of gravity, and tether i coiled on the winch, installed on a gimbal. The local reference system D_i is depicted, too.

Regarding measurement aspects, we assume that each drone is equipped with local sensors that acquire its attitude, three-dimensional inertial position and velocity, and the winch angular position and speed. Such sensors are nowadays available with high accuracy at relatively low price, e.g. integrated in an inertial measurement unit (IMU). Moreover, each drone is assumed to also acquire the inertial position of the next one in the chain. This information can be transmitted either through the tether or via wireless communication, or both. The ground station is assumed to acquire the local winch position and speed, plus the inertial position vectors and yaw angle of all the drones in the chain, again transmitted either via tether or wireless.

The controller of the ground station can directly manipulate the torque of the ground winch, moreover it is in charge of acting as supervisory controller,

by sending reference values of position and yaw angle to each drone in the chain. The electronic control unit of each drone is in charge of tracking such references by manipulating the four rotor speeds (we assume here ideal control of the propellers, such that the commanded speed values correspond to the actual ones). Moreover, each local controller must also ensure that the tether connected to the next drone in the chain is neither too slack (with consequent possible entanglement) nor taut, which might compromise the stability of the whole system. Such a tether adjustment is achieved by manipulating locally the winch torque.

In general, the overall control objective for the described system is to optimize a desired performance criterion, subject to operational constraints on the geometrical configuration of the whole chain. Such operational constraints depend on the specific system topology (number of drones, maximum length of the tethers, etc.) and application (type of task and environment). In this paper, we provide an example of possible performance criterion and operational constraints pertaining to a chain of three drones, see Sections 4.2 and 5, but the modeling and control design approaches described in the remainder are general and can be therefore applied to systems with a different number of elements and other control objectives.

3 System model

3.1 Coordinate systems and notation

We start by introducing an inertial right-handed reference system $G \doteq (X, Y, Z)$, centered at the ground station with the $Z-$axis pointing upwards, see Figure 1-(a). The tethered robotic system features $M \in \mathbb{N}$ drones, identified by a progressive index $i = 1, \ldots, M$ starting from the one attached to the ground station. A local body frame for each drone is also considered, denoted by $D_i \doteq (x_i, y_i, z_i)$, see Figure 1-(b). The attitude of each drone with respect to the inertial system G is provided by its Euler angles, i.e. yaw $\psi_i(t)$, pitch $\theta_i(t)$, and roll $\varphi_i(t)$, where t is the continuous time variable. The Euler angles define the rotation matrix (see e.g. [19]):

$$R_i(t) = \begin{bmatrix} \mathrm{c}(\psi_i)\mathrm{c}(\theta_i) & \mathrm{c}(\psi_i)\mathrm{s}(\theta_i)\mathrm{s}(\varphi_i) - \mathrm{s}(\psi_i)\mathrm{c}(\varphi_i) & \mathrm{c}(\psi_i)\mathrm{s}(\theta_i)\mathrm{c}(\varphi_i) + \mathrm{s}(\psi_i)\mathrm{s}(\varphi_i) \\ \mathrm{s}(\psi_i)\mathrm{c}(\theta_i) & \mathrm{s}(\psi_i)\mathrm{s}(\theta_i)\mathrm{s}(\varphi_i) + \mathrm{c}(\psi_i)\mathrm{c}(\varphi_i) & \mathrm{s}(\psi_i)\mathrm{s}(\theta_i)\mathrm{c}(\varphi_i) - \mathrm{c}(\psi_i)\mathrm{s}(\varphi_i) \\ -\mathrm{s}(\theta_i) & \mathrm{c}(\theta_i)\mathrm{s}(\varphi_i) & \mathrm{c}(\theta_i)\mathrm{c}(\varphi_i) \end{bmatrix}. \quad (1)$$

In (1), for the sake of space we omitted the time dependency of the Euler angles and we adopted the notation $\mathrm{c}(\cdot) \doteq \cos(\cdot)$ and $\mathrm{s}(\cdot) \doteq \sin(\cdot)$. Matrix $R_i(t)$ is used to translate a vector from the inertial coordinates, G, to the local ones, D_i, and vice-versa by using $R_i^{-1} = R_i^\top$ (where $^\top$ is the matrix transpose operation). The position and velocity of each drone in the inertial system are denoted by ${}_G\mathbf{p}_i(t)$, ${}_G\dot{\mathbf{p}}_i(t)$, where $\dot{p}(t) \doteq dp(t)/dt$, the boldface symbol denotes a three-dimensional vector, and the preceding subscript indicates the reference coordinate system used to compute the vector's components. Thus, for example we have:

$${}_G\dot{\mathbf{p}}_i(t) = R_i^\top \, {}_{D_i}\dot{\mathbf{p}}_i(t).$$

The components of each vector are indicated with the corresponding non-bold letter, preceded by the coordinate axis, e.g. ${}_G\dot{\mathbf{p}}_i(t) = ({}_X\dot{p}_i(t), {}_Y\dot{p}_i(t), {}_Z\dot{p}_i(t))$.

All vectors are assumed to be columns, unless otherwise stated.
An exception to the vector notation introduced so far is represented by the components of the angular velocity vector of each drone in local coordinates. In fact, to be consistent with a large portion of the literature on flight control, we denote with $(p_i(t),\, q_i(t),\, r_i(t))$ the angular velocities of the i^{th} drone about its local x_i, y_i, and z_i axes, respectively. The time derivatives of the Euler angles are linked to the angular velocity of the drone by (see e.g. [19]):

$$\begin{bmatrix} \dot{\varphi} \\ \dot{\theta} \\ \dot{\psi} \end{bmatrix} = \begin{bmatrix} 1 & \sin(\varphi_i)\tan(\theta_i) & \cos(\varphi_i)\tan(\theta_i) \\ 0 & \cos(\varphi_i) & -\sin(\varphi_i) \\ 0 & \sin(\varphi_i)/\cos(\theta_i) & \cos(\varphi_i)/\cos(\theta_i) \end{bmatrix} \begin{bmatrix} p_i \\ q_i \\ r_i \end{bmatrix}, \tag{2}$$

where we omitted again the time dependency for the sake of space.

3.2 Winch and tether models

The winches along the chain are also identified by the progressive index i, where $i = 0$ corresponds to the ground station, and the subsequent $i = 1, \ldots, M-1$ match the indexes used for the drones. The different sections of tether are identified by the index of the corresponding winch, so for example the tether connecting the ground station to the first drone is denoted with $i = 0$, and so on. We denote with $\vartheta_i(t)$, $\dot{\vartheta}_i(t)$ the angular position and velocity of the i^{th} winch. We assume that when $\vartheta_i(t) = 0$, the whole available length of tether is coiled on the winch. We further assume that the tether can be fully coiled on a single layer, i.e. the effective radius of the winch does not depend on the length of unreeled tether. Then, the mass of the winch is computed as:

$$m_{\text{w},i}(t) = \underline{m}_{\text{w},i} + (\bar{l}_i - r_{\text{e},i}\vartheta_i(t))\rho_{\text{t},i}, \tag{3}$$

where $\underline{m}_{\text{w},i}$ is the mass of the winch without tether, ρ_{t} is the mass of the tether per unit of length, $\bar{l}_i$ is the maximum tether length, and $r_{\text{e},i}$ is the winch radius (i.e. the product $r_{\text{e},i}\vartheta_i(t)$ represents the length of tether that has been reeled-out of the winch). Note that in principle we allow the different tethers to have different mass for the same length; this is reasonable since with a series connection each tether has to carry the sum of the currents consumed by all the subsequent drones along the chain, and its diameter shall be thus dimensioned accordingly in order to limit the voltage drop. Considering a hollow drum with inner radius $r_{\text{i},i}$, the moment of inertia of each winch is approximated as:

$$J_{\text{w},i}(t) = \frac{1}{2} m_{\text{w},i}(t)\left(r_{\text{e},i}^2 + r_{\text{i},i}^2\right). \tag{4}$$

The viscous friction coefficient of the winch is assumed constant and denoted with $\beta_{\text{w},i}$. The winch torque (control input) is denoted with $u_{\text{w},i}(t)$ and it is physically limited in the interval $[\underline{u}_{\text{w},i},\, \overline{u}_{\text{w},i}]$. Finally, the pulling force vector ${}_G\mathbf{F}_{\text{t},i}(t)$ exerted by the tether is computed on the basis of its stiffness $K_{\text{t},i}$ (assumed constant for simplicity), and its elongation $e_{\text{t},i}(t)$, computed as:

$$e_{\text{t},i}(t) = \max\left(0, \|{}_G\mathbf{p}_{i+1}(t) -_G \mathbf{p}_i(t)\|_2 - r_{\text{e},i}\vartheta_i(t)\right). \tag{5}$$

The tether forces are then derived as:

$$ {}_G\mathbf{F}_{\mathrm{t},i}(t) = K_{\mathrm{t},i} e_{\mathrm{t},i}(t) \frac{{}_G\mathbf{p}_{i+1}(t) - {}_G\,\mathbf{p}_i(t)}{\|{}_G\mathbf{p}_{i+1}(t) - {}_G\,\mathbf{p}_i(t)\|_2}, \tag{6} $$

where ${}_Gp_0 = (0,0,0)$ is the position of the ground station. Note that in (6) the force vector is assumed to be directed along the line passing through the centers of gravity of the two elements to which the tether is linked, i.e. we neglect the presence of the gimbal when computing the force orientation (but not when computing the moment induced by the tether, as shown in Section 3.3). This is reasonable, since the tether length is usually much larger than the distance between the gimbal and the drone's center of gravity.
From the equilibrium of moments around the rotational axis, the equation of motion for each winch $i = 0, \ldots, M-1$ is then:

$$ \ddot{\vartheta}_i(t) = \frac{1}{J_{\mathrm{w},i}(t)} \left(r_{\mathrm{e},i} \|{}_G\mathbf{F}_{\mathrm{t},i}\|_2 - \beta_{\mathrm{w},i}\dot{\vartheta}_i(t) + u_{\mathrm{w},i}(t) \right). \tag{7} $$

Finally, regarding the other forces exerted by the tethers on the drones, we neglect the aerodynamic drag, under the assumption of low apparent wind speed (i.e. little absolute wind, and relatively slow movement of the drones), and we account for the weight of each tether by adding half of its mass to the mass of the two drones connected to its extremes, as shown in the next Section. In particular, the mass $m_{\mathrm{t},i}(t)$ of the tether connecting drone i to drone $i+1$ is:

$$ m_{\mathrm{t},i}(t) = r_{\mathrm{e},i}\vartheta_i(t)\rho_{\mathrm{t},i}. \tag{8} $$

3.3 Quadrotor helicopter model

We consider a rather standard model to describe the drones' dynamics, see e.g. [5], which we augment by adding the terms (forces and moments) pertaining to the interactions with the tethers, as well as the time varying mass due to tether reeling. We start by introducing the lift forces and drag torques contributed by the four rotors:

$$ \begin{array}{rcl} L_{j,i}(t) & = & b_i\,\Omega_{j,i}^2, \quad j = 1, \ldots, 4 \\ T_{j,i}(t) & = & d_i\,\Omega_{j,i}^2, \quad j = 1, \ldots, 4 \end{array} \tag{9} $$

where the index j refers to the rotors according to Figure 1-(b), $\Omega_{j,i}$ is the rotational speed of the j^{th} rotor of the i^{th} drone, and b_i, d_i are the rotors' lift and drag coefficients for the i^{th} drone. We can now linearly combine the four lift forces and drag torques into four inputs, $u_{1,i}(t), \ldots, u_{4,i}(t)$, corresponding respectively to the total lift along z_i axis and to yaw moments around the x_i, y_i, and z_i axes (see Figure 1-(b)):

$$ \begin{array}{rcl} u_{1,i}(t) & = & \sum_{j=1}^{4} L_{j,i}(t) \\ u_{2,i}(t) & = & a_{\mathrm{r},i}\,(L_{4,i} - L_{2,i}) \\ u_{3,i}(t) & = & a_{\mathrm{r},i}\,(L_{3,i} - L_{1,i}) \\ u_{4,i}(t) & = & (T_{2,i} + T_{4,i}) - (T_{1,i} + T_{3,i})\,. \end{array} \tag{10} $$

In (10), $a_{\mathrm{r},i}$ is the distance between each rotor and the drone center of gravity. Finally, we compute the total drone mass as:

$$ m_{\mathrm{d},i}(t) = \underline{m}_{\mathrm{d},i} + m_{\mathrm{w},i}(t) + 0.5 m_{\mathrm{t},i}(t) \tag{11} $$

where $\underline{m}_{\mathrm{d},i}$ is the drone mass without winch and tethers, and $m_{\mathrm{w},i}(t)$, $m_{\mathrm{t},i}(t)$ are computed according to (3), (8), respectively.
We can now introduce the equations of motion for the tethered drone (where we omit the time dependence for the sake of space):

$$ {}_G\ddot{\mathbf{P}}_i = \frac{1}{m_{\mathrm{d},i}} \left(R_i^\top \begin{bmatrix} 0 \\ 0 \\ u_{1,i} \end{bmatrix} + ({}_G\mathbf{F}_{\mathrm{t},i} - {}_G\,\mathbf{F}_{\mathrm{t},i-1}) \right) - \begin{bmatrix} 0 \\ 0 \\ g \end{bmatrix} \tag{12a} $$

$$ \dot{p}_i = \frac{I_{y_i} - I_{z_i}}{I_{x_i}} q_i\, r_i + \frac{u_{2,i}}{I_{x_i}} - \frac{J_{\mathrm{p},i}}{I_{x_i}} q_i\, \Omega_{\mathrm{r},i} + d_{\mathrm{w,i}\ y_i} F_{\mathrm{t},i} \tag{12b} $$

$$ \dot{q}_i = \frac{I_{z_i} - I_{x_i}}{I_{y_i}} p_i\, r_i + \frac{u_{3,i}}{I_{y_i}} + \frac{J_{\mathrm{p},i}}{I_{y_i}} p_i\, \Omega_{\mathrm{r},i} - d_{\mathrm{w,i}\ x_i} F_{\mathrm{t},i} + \frac{u_{\mathrm{w},i}}{I_{y_i}} p_i \tag{12c} $$

$$ \dot{r}_i = \frac{I_{x_i} - I_{y_i}}{I_{z_i}} p_i\, q_i + \frac{u_{4,i}}{I_{z_i}} \tag{12d} $$

Where g is the gravity acceleration, I_{x_i}, I_{y_i}, I_{z_i} are the drone rotational moments of inertia, $J_{\mathrm{p},i}$ is the moment of inertia of each propeller/motor on the drone, and $d_{\mathrm{w,i}}$ is the distance between the center of gravity and the point where the i^{th} tether leaves its winch (see Figure 1-(b)). The model (12) is derived using Newton's law and it includes the effects of the tethers' pulling forces, the torque applied by the onboard winch, and the changing mass due to the time-varying lengths of the tethers connected to each drone. The main simplifying assumptions, which will be lifted in future research, are the absence of tether drag forces and the use of constant moments of inertia for the drones, i.e. independent from the length of the tethers and (consequently) from the winch mass. Altogether, equations (1)-(12) allow one to set up and simulate STEM with arbitrary number of drones. In the next Section, we present an approach to design a control system for this class of tethered UAVs.

4 Control design

We propose a hierarchical control approach as depicted in Figure 2, where local controllers in the inner loop are in charge of tracking the reference position and yaw values provided by the supervisory controller.

4.1 Local controllers

We design decoupled controllers for each winch and drone, i.e. the rotors' speeds are computed independently from the winch torque. A layout of the local controllers is shown in Figure 3.

Regarding the winch controller, the goal is to regulate the tether length in order to limit tether sag, while at the same time avoiding that the tether becomes taut. In order to achieve this goal, we consider the measured distance between winch i and drone $i+1$, and set a reference winch position $\vartheta_i^{\mathrm{ref}}(t)$ such that the corresponding tether length is larger than this distance by a quantity $\Delta l_{\mathrm{t},i} > 0$, which is a design parameter:

$$ \vartheta_i^{\mathrm{ref}}(t) = \left(\|{}_G\mathbf{p}_{i+1}(t) - {}_G\,\mathbf{p}_i(t)\|_2 + \Delta l_{\mathrm{t},i} \right) / r_{\mathrm{e},i}. \tag{13} $$

Then, we compute the winch torque using a linear, static state feedback law:

$$ u_{\mathrm{w},i}(t) = K_{\mathrm{w},i} \begin{bmatrix} \vartheta_i^{\mathrm{ref}}(t) - \vartheta_i(t) \\ -\dot{\vartheta}_i(t) \end{bmatrix}. \tag{14} $$

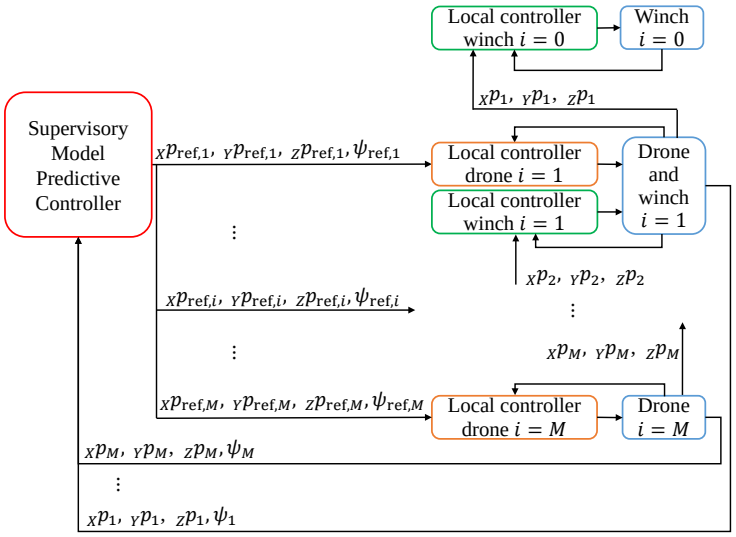

Figure 2: Layout of the overall control structure.

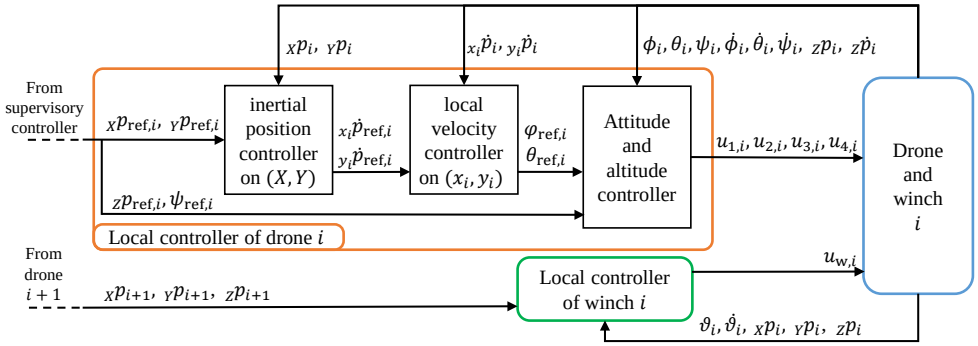

Figure 3: Layout of the local controllers for each drone and winch.

where the gain vector $K_{\mathrm{w},i}$ is computed via pole-placement ([7]) using the model obtained from (7) with ${}_G\mathbf{F}_{\mathrm{t},i} = 0$, i.e. assuming that the tether is not taut. The winch torque is finally saturated in the interval $[\underline{u}_{\mathrm{w}}, \overline{u}_{\mathrm{w}}]$ to comply with physical constraints on the actuator.

About the drone controller, several techniques have been proposed in the literature, many of them exploiting differential flatness properties (see e.g. [5] and [16]). Here, we propose a rather straightforward approach where the drone controller is itself a hierarchical one, with three nested loops as shown in Figure 3. In the innermost control loop, a static, multi-variable linear controller manipulates the rotor speeds in order to track reference attitude (i.e. roll, pitch and yaw angles) and altitude values. This controller is designed using the following linear model, which can be easily derived from (2) and (12) assuming that pitch and roll angles take relatively small values (such that one can linearize their trigonometric functions), that the tethers are not taut, and considering a nominal mass value $m_{\mathrm{d,i}}^{\mathrm{nom}}$ for the drone (recall that the mass changes during

operation depending on the tethers' reeling motion):

$$ {}_Z\ddot{p}_i(t) = \frac{u_{1,i}(t)}{m_{\mathrm{d,i}}^{\mathrm{nom}}} - g + d_{z_i}(t) \tag{15a} $$

$$ \ddot{\varphi}_i(t) = \frac{u_{2,i}(t)}{I_{x_i}} + d_{\varphi_i}(t) \tag{15b} $$

$$ \ddot{\theta}_i(t) = \frac{u_{3,i}(t)}{I_{y_i}} + d_{\theta_i}(t) \tag{15c} $$

$$ \ddot{\psi}_i(t) = \frac{u_{4,i}(t)}{I_{z_i}} + d_{\theta_i}(t). \tag{15d} $$

In (15b)-(15d), the additive terms $d_{z_i}(t)$, $d_{\varphi_i}(t)$, $d_{\theta_i}(t)$, $d_{\theta_i}(t)$ account for the errors induced by the small-angles approximation and by the neglected couplings between the rotational modes of the drones (compare (12)). Such terms can be realistically assumed to be bounded and, if the performed maneuvers are not too harsh compared with the available rotors' lift and drag, to be negligible with respect to the control input. The linear model (15) allows one to carry out a very simple and effective control design. A similar modeling approach has been also successfully tested in experiments with a tethered glider, see [4]. The controller in the inner control loop takes the following form:

$$ \begin{bmatrix} u_{1,i}(t) \\ u_{2,i}(t) \\ u_{3,i}(t) \\ u_{4,i}(t) \end{bmatrix} = K_{\mathrm{d},i}^{\mathrm{il}} \begin{bmatrix} {}_Zp_{\mathrm{ref},i}(t) - {}_Z\,p_i(t) \\ -{}_Z\dot{p}_i(t) \\ \varphi_{\mathrm{ref},i}(t) - \varphi_i(t) \\ -\dot{\varphi}_i(t) \\ \theta_{\mathrm{ref},i}(t) - \theta_i(t) \\ -\dot{\theta}_i(t) \\ \psi_{\mathrm{ref},i}(t) - \psi_i(t) \\ -\dot{\psi}_i(t) \end{bmatrix} + \begin{bmatrix} m_{\mathrm{d,i}}^{\mathrm{nom}}\, g \\ 0 \\ 0 \\ 0 \end{bmatrix} \tag{16} $$

where the static gain matrix $K_{\mathrm{d},i}^{\mathrm{il}} \in \mathbb{R}^{4\times 8}$ is computed again via pole-placement based on the model (15). Note that the (nominal) gravity force is compensated with a feed-forward contribution in (16). The altitude controller in (16) is directly used to track a desired vertical position ${}_Zp_{\mathrm{ref},i}$ in the inertial frame (see Figure 3). Similarly, the yaw angle controller is used directly to track the reference yaw rate $\psi_{\mathrm{ref},i}(t)$. On the other hand, to compute the reference roll and pitch angles a second controller is employed, which forms the middle control loop of Figure 3. In particular, this controller computes the reference attitude in order to track a desired velocity vector, expressed in the local $(x_i,\, y_i)$ coordinates. The design is based on the following linearized model, which is obtained from (1), (12a) and (16) under the same simplifying assumptions considered to derive (15) (i.e. small pitch and roll angles):

$$ \begin{aligned} {}_{x_i}\ddot{p}_i(t) &= g\theta_{\mathrm{ref},i}(t) + d_{x_i}(t) \\ {}_{y_i}\ddot{p}_i(t) &= -g\varphi_{\mathrm{ref},i}(t) + d_{y_i}(t), \end{aligned} \tag{17} $$

where, similarly to (15), the terms $d_{x_i}(t)$, $d_{y_i}(t)$ account for neglected dynamics, for the tracking errors between $\varphi_{\mathrm{ref},i}$, $\theta_{\mathrm{ref},i}$ and $\varphi_i(t)$, $\theta_i(t)$, and for the discrepancy between the total lift force, $u_{1,i}$, and the nominal weight force, $m_{\mathrm{d,i}}^{\mathrm{nom}}\, g$

(compare (12a) and (16)). The reference roll and pitch angles are then computed as:

$$\begin{bmatrix} \theta_{\mathrm{ref},i}(t) \\ \varphi_{\mathrm{ref},i}(t) \end{bmatrix} = K_{\mathrm{d},i}^{\mathrm{ml}} \begin{bmatrix} {}_{x_i}\dot{p}_{\mathrm{ref},i}(t) - {}_{x_i}\dot{p}_i(t) \\ -\left({}_{y_i}\dot{p}_{\mathrm{ref},i}(t) - {}_{y_i}\dot{p}_i(t) \right) \end{bmatrix} \tag{18}$$

where $K_{\mathrm{d},i}^{\mathrm{ml}}$ is computed with pole-placement based on the model (17) (the minus sign in the second row of the error vector in (18) is due to the different signs of the gains in (17)). In order to comply with the assumption of small pitch and roll angles, the reference values computed in (18) are then saturated within the intervals $[\underline{\theta}_{\mathrm{ref}}, \overline{\theta}_{\mathrm{ref}}]$, $[\underline{\varphi}_{\mathrm{ref}}, \overline{\varphi}_{\mathrm{ref}}]$, which are tuning parameters as well.
At the outermost level, another static linear controller computes the reference velocity vector in order to track a desired position in the inertial coordinate frame G. We employ a simple kinematic model to design such a controller:

$$\begin{array}{rcl} {}_X\dot{p}_i(t) & = & {}_X\dot{p}_{\mathrm{ref},i}(t) + e_{X_i}(t) \\ {}_Y\dot{p}_i(t) & = & {}_Y\dot{p}_{\mathrm{ref},i}(t) + e_{Y_i}(t), \end{array} \tag{19}$$

where $e_{X_i}(t)$, $e_{Y_i}(t)$ are the tracking errors of the velocity components under the action of controllers (16) and (18), rotated to the inertial coordinate system. The outer controller reads:

$$\begin{bmatrix} {}_X\dot{p}_{\mathrm{ref},i}(t) \\ {}_Y\dot{p}_{\mathrm{ref},i}(t) \end{bmatrix} = K_{\mathrm{d},i}^{\mathrm{ol}} \begin{bmatrix} {}_Xp_{\mathrm{ref},i}(t) - {}_Xp_i(t) \\ {}_Yp_{\mathrm{ref},i}(t) - {}_Yp_i(t) \end{bmatrix} \tag{20}$$

where $K_{\mathrm{d},i}^{\mathrm{ol}}$ is also computed with pole-placement based on the model (19). The reference speed values are finally converted from the inertial to the local coordinate system, in order to be usable by the middle-level controller (18):

$$\begin{bmatrix} {}_{x_i}\dot{p}_{\mathrm{ref},i}(t) \\ {}_{y_i}\dot{p}_{\mathrm{ref},i}(t) \end{bmatrix} = \begin{bmatrix} \cos\left(\psi_i(t)\right) & \sin\left(\psi_i(t)\right) \\ -\sin\left(\psi_i(t)\right) & \cos\left(\psi_i(t)\right) \end{bmatrix} \begin{bmatrix} {}_X\dot{p}_{\mathrm{ref},i}(t) \\ {}_Y\dot{p}_{\mathrm{ref},i}(t) \end{bmatrix} \tag{21}$$

Summing up, all of the local controllers are given by static linear feedback laws (with the exception of the nonlinear transformation (21)). All of them are implemented in discrete time with a sampling period T_{l}, chosen according to standard criteria based on the system dynamics and the desired closed-loop bandwidth ([7]). The main tuning parameters of the local controllers are the poles of the corresponding closed-loop systems.

4.2 Supervisory controller

As shown in Figure 2, the reference position and yaw for all of the drones are computed by a centralized supervisory controller exploiting a Model Predictive Control (MPC) approach, see e.g. [6]. The supervisory controller receives the position and yaw measurements from all the drones and it updates the corresponding reference values with a sampling period $T_{\mathrm{u}} \geq T_{\mathrm{l}}$, by solving at each time step a finite horizon optimal control problem (FHOCP) in a receding-horizon fashion. Let us denote with $k \in \mathbb{N}$ the discrete-time variable corresponding to the sampling period T_{u}. The discrete-time models employed to formulate the FHOCP are based on the closed-loop position and yaw dynamics of each drone under the action if its local controller. In particular, in order to reduce the computational burden and to obtain a convex optimization problem,

we use simple linear prediction models of the following form (obtained via the Euler method):

$$\begin{aligned} {}_G\mathbf{p}_i(k+1) &= (1 - T_{\mathrm{u}}\omega_{\mathbf{p},i})\,{}_G\mathbf{p}_i(k) + T_{\mathrm{u}}\omega_{\mathbf{p},i}\,{}_G\mathbf{p}_{\mathrm{ref},i}(k) \\ \psi_i(k+1) &= (1 - T_{\mathrm{u}}\omega_{\psi,i})\,\psi_i(k) + T_{\mathrm{u}}\omega_{\psi,i}\,\psi_{\mathrm{ref},i}(k) \end{aligned} \tag{22}$$

where $i = 1, \ldots, M$ and the parameters $\omega_{\mathbf{p},i}$, $\omega_{\psi,i}$ correspond to the dominant poles of the closed-loop response of each drone i. A good guess of these parameters can be obtained based on the closed loop transfer function obtained with the local controllers applied to the related design models (15), (17), (19). Such a starting guess can then be refined by further tuning via simulations/experiments. In (22) we implicitly assume that the MPC sampling frequency is chosen to be sufficiently larger than the dominant poles, such that the discrete time models match well with the real closed-loop behavior of the drones.

Let us now define the vectors $v(k)$, $\Delta v(k)$ and $w(k)$ comprising, respectively, the reference values, their one-step change, and the measured feedback variables for all the drones:

$$\begin{aligned} v(k) &\doteq \left[{}_G\mathbf{p}_{\mathrm{ref},1}(k), \psi_{\mathrm{ref},1}(k), \ldots, {}_G\,\mathbf{p}_{\mathrm{ref},M}(k), \psi_{\mathrm{ref},M}(k)\right]^\top \in \mathbb{R}^{4M} \\ \Delta v(k) &\doteq v(k) - v(k-1) \in \mathbb{R}^{4M} \\ w(k) &\doteq \left[{}_G\mathbf{p}_1(k), \psi_1(k), \ldots, {}_G\,\mathbf{p}_M(k), \psi_M(k)\right]^\top \in \mathbb{R}^{4M} \end{aligned}$$

Vector $v(k)$ includes all the manipulated variables from the perspective of the supervisory controller. With straightforward manipulations, we can re-write the models (22) as:

$$w(k+1) = f(w(k), v(k)), \tag{23}$$

where function f is a linear combination of its arguments, compare eq. (22). Let us further denote with $v(j|k)$, $\Delta v(j|k)$ and $w(j|k)$ the values of v, Δv and w predicted at time instant k, pertaining to j steps in the future. At each time step, the MPC law is computed by solving the following FHOCP:

$$\min_{v(0|k),\ldots,v(N-1|k)} \sum_{j=0}^{N-1} \left(\ell(w(j|k), \Delta v(j|k))\right) + g(w(N|k)) \tag{24a}$$

subject to

$$w(j+1|k) = f(w(j|k), v(j|k)),\ j = 0, \ldots, N-1 \tag{24b}$$

$$w(0|k) = w(k) \tag{24c}$$

$$h(w(j|k), v(j|k), \Delta v(j|k)) \leq 0,\ j = 1, \ldots, N-1. \tag{24d}$$

In (24), $N \in \mathbb{N}$ is the prediction horizon, $\ell : \mathbb{R}^{8M} \to \mathbb{R}^+$ is the so-called stage cost, $g : \mathbb{R}^{4M} \to \mathbb{R}^+$ the terminal cost, and $h : \mathbb{R}^{12M} \to \mathbb{R}^P$ is a vector-valued function collecting P inequality constraints (equation (24d) shall be read as element-wise inequalities). All of these parameters and functions are chosen by the control designer. Since the model (23) is linear, if the constraints, stage cost and terminal cost are selected as convex functions in their arguments, the FHOCP (24) results to be a convex optimization problem, for which efficient solution algorithms exist (see e.g. [1]).

Up to this point, we decidedly employed a general formulation without specific cost and constraint functions, since these choices depend largely on the

considered STEM configuration (number of drones, maximum length of tethers, etc.) and control objective. We provide next a possible choice of cost and constraint functions, which we employed to carry out the numerical simulations described in the next Section. We consider a chain of $M = 3$ drones, and the control objective is to track a desired configuration (position and attitude) of the last drone, issued to the ground station controller by an external user (e.g. a human pilot). Denoting with ${}_G\mathbf{p}_{\text{des},3}$, $\psi_{\text{des},3}$ such a desired configuration, we select the stage and terminal costs and the constraints as:

$$\begin{aligned} \ell(w, \Delta v) &= \|{}_G\mathbf{p}_{\text{des},3} - {}_G\,\mathbf{p}_3\|_2^2 + \alpha(\psi_{\text{des},3} - \psi_3)^2 + \beta \Delta v^\top \Delta v \\ g(w) &= \|{}_G\mathbf{p}_{\text{des},3} - {}_G\,\mathbf{p}_3\|_2^2 + \alpha(\psi_{\text{des},3} - \psi_3)^2 \end{aligned} \tag{25}$$

$$h(w, v, \Delta v) = \begin{bmatrix} \|({}_X\mathbf{p}_1, {}_Y\mathbf{p}_1)\|_\infty - D \\ |({}_Z\mathbf{p}_2 - {}_Z\,\mathbf{p}_1)| - D \\ {}_Z\mathbf{p}_3 - {}_Z\,\mathbf{p}_1 + C \\ {}_Z\mathbf{p}_3 - {}_Z\,\mathbf{p}_2 + C \\ \|({}_X\mathbf{p}_3 - {}_X\,\mathbf{p}_2,\ {}_Y\mathbf{p}_3 - {}_Y\,\mathbf{p}_2)\|_\infty - D \\ \|{}_G\mathbf{p}_1\|_2 - \bar{l}_0 \\ \|{}_G\mathbf{p}_2 - {}_G\,\mathbf{p}_1\|_2 - \bar{l}_1 \\ \|{}_G\mathbf{p}_3 - {}_G\,\mathbf{p}_2\|_2 - \bar{l}_2 \\ |\Delta v_1| - \overline{\Delta v}_1 \\ \vdots \\ |\Delta v_{4L}| - \overline{\Delta v}_{4L} \end{bmatrix}, \tag{26}$$

where $\alpha > 0$, $\beta > 0$ are cost weighting factors, $C > 0$, $D > 0$ are the maximum allowed misalignments between one drone and the next one (along selected directions), and $\overline{\Delta v}_j$, $j = 1, \ldots, 4M$ are the maximum allowed changes of each element of vector $\Delta v(k)$ (i.e. rate constraints on vector $v(k)$).
The rationale behind (25)-(26) is the following: we want to track the desired position and yaw of the last drone, while at the same time keeping the (X, Y) position of the first drone within a square of side $2D$ centered at the ground station, the Z position of the second drone within $\pm D$ from that of the first drone, and the Z position of both the first and second drone higher than that of the last one by the quantity C. Moreover, the (X, Y) position of the second drone shall be kept in a square of side $2D$ centered at the third drone. Finally, the distance between any two subsequent drones (and between the first one and the ground station) shall be smaller than the corresponding maximum tether length. An example of results obtained using such cost and constraint functions is presented in the next Section.

5 Simulation results

We consider the three-drone STEM described above, with model parameters reported in Table 1. In particular, the basis for the drones' parameters is taken from [9], where we reduced the minimum drone mass (i.e. without winch) by removing the batteries' mass. The drone mass can change between 0.65 kg (drone plus winch with tether fully reeled-out) and about 0.85 kg (drone plus winch with tether fully reeled-in). We show the simulation results pertaining to a maneuver where the three drones start with zero attitude, linear velocity

Table 1: Simulation study with three-drone STEM: model parameters. All drones ($i = 1, 2, 3$) and winches ($i = 0, 1, 2$) have the same parameter values.

Drones		
$\underline{m}_{\mathrm{d},i}$	0.455	kg
g	9.81	$\mathrm{m/s^2}$
b_i	$7.2\ 10^{-5}$	$\mathrm{N\,s^2/rad^2}$
d_i	10^{-5}	$\mathrm{Nm\,s^2/rad^2}$
$a_{\mathrm{r},i}$	0.3	m
$J_{\mathrm{p},i}$	$3.4\ 10^{-5}$	$\mathrm{kg\,m^2}$
I_{x_i}	$4.3\ 10^{-3}$	$\mathrm{kg\,m^2}$
I_{y_i}	$4.3\ 10^{-3}$	$\mathrm{kg\,m^2}$
I_{z_i}	$4.3\ 10^{-3}$	$\mathrm{kg\,m^2}$
Winches and tethers		
$\underline{m}_{\mathrm{w},i}$	$2\ 10^{-1}$	kg
ρ_{t}	$1.2\ 10^{-2}$	kg/m
$\overline{l}_i$	16	m
$r_{\mathrm{e},i}$	$5\ 10^{-2}$	m
$\beta_{\mathrm{w},i}$	$5\ 10^{-3}$	Nm s/rad
$\underline{u}_{\mathrm{w},i}$, $\overline{u}_{\mathrm{w},i}$	$\pm 4\ 10^{-1}$	Nm
$K_{\mathrm{t},i}$	10^3	N/m
$d_{\mathrm{w,i}}$	10^{-1}	m

Table 2: Simulation study with three-drone STEM: local controllers' parameters. All drones ($i = 1, 2, 3$) and winches ($i = 0, 1, 2$) have the same parameter values.

Sampling time		
T_{l}	10^{-2}	s
Drones		
$m_{\mathrm{d,i}}^{\mathrm{nom}}$	$5.5\ 10^{-1}$	kg
$K_{\mathrm{d},i}^{\mathrm{ml}}$	$8.1\ 10^{-1}$	rad s/m
$K_{\mathrm{d},i}^{\mathrm{ol}}$	2.2	1/s
$\underline{\theta}_{\mathrm{ref}}$, $\overline{\theta}_{\mathrm{ref}}$	$\pm 5.2\ 10^{-1}$	rad
$\underline{\varphi}_{\mathrm{ref}}$, $\overline{\varphi}_{\mathrm{ref}}$	$\pm 5.2\ 10^{-1}$	rad
Winches		
$\Delta l_{\mathrm{t},i}$	0.5	m
$K_{\mathrm{w},i}$	[2.2 -0.08]	

and angular velocity, and with the following initial position values in m:

$$ {}_G\mathbf{p}_1 = \begin{bmatrix} 0 \\ 0 \\ 1 \end{bmatrix}, \ {}_G\mathbf{p}_2 = \begin{bmatrix} 0.5 \\ 0.5 \\ 1 \end{bmatrix}, \ {}_G\mathbf{p}_3 = \begin{bmatrix} 0.5 \\ 0.5 \\ 0.2 \end{bmatrix} $$

Regarding the winches, they are also initialized with zero angular speed, and initial tether lengths $r_{\mathrm{e},0}\vartheta_0(0) = 1.5\,\mathrm{m}$, $r_{\mathrm{e},1}\vartheta_1(0) = 1.2\,\mathrm{m}$, $r_{\mathrm{e},2}\vartheta_2(0) = 1.3\,\mathrm{m}$, i.e. slightly larger than the corresponding initial distances between each winch

Table 3: Simulation study with three-drone STEM: MPC parameters.

T_{u}	$2.5\ \ 10^{-1}$	s
$\omega_{\mathbf{p},i}$	2	rad/s
$\omega_{\psi,i}$	1	rad/s
N	10	
α	10^{-4}	
β	10^{-3}	
D	3	m
C	0.5	m

and the next drone in the chain. The desired target for drone $i = 3$ is the position vector ${}_G\mathbf{p}_{\mathrm{des},3} = [10,\, 17,\, 2]^\top$ m and yaw angle $\psi_{\mathrm{des},3} = \pi$ rad. We implemented the local and supervisory controllers as described in Section 4, with the parameters reported in Tables 2-3. Regarding the local controllers, the scalar gains for the middle and upper control loops are shown in Table 2, while the matrix gain for the inner loop (attitude and altitude controllers) is:

$$K_{\mathrm{d},i}^{\mathrm{il}} = \begin{bmatrix} 60.4 & 0 & 0 & 0 & 11.5 & 0 & 0 & 0 \\ 0 & 1.06 & 0 & 0 & 0 & 0.13 & 0 & 0 \\ 0 & 0 & 1.06 & 0 & 0 & 0 & 0.13 & 0 \\ 0 & 0 & 0 & 2.55 & 0 & 0 & 0 & 0.3245 \end{bmatrix}$$

Regarding the reference rate constraints in (26), we impose a maximum rate of change of the reference position of 12 m/s. The corresponding entries $\overline{\Delta v}_j$, $j = 1, \ldots, 4L$ of vector $\overline{\Delta v}$ are not shown in Table 3 for the sake of brevity. We solved the FHOCP using the standard Matlab® function `fmincon`. Figure 4 presents the trajectories of the tethered drones in the inertial coordinate system G. The supervisory controller works on the constraints in order to quickly reach the target position In particular, after the first transient the reference positions of drones $i = 2$ and $i = 3$ are kept consistently on the boundary of the constraint set. Figure 5 shows the time courses of the position components of drone $i = 3$ in the inertial frame, together with the references provided by the supervisory controller. The course of the attitude (reference and actual) of the same drone is depicted in Figure 6. The different sampling frequency of the roll and pitch references (computed by the local controller) an the yaw reference (computed by the MPC law) is evident. Moreover, it can be noted that the roll and pitch angles are always kept at relatively small values, so that the linear models employed for control design are quite accurate. Finally, the winch control performances are presented in Figure 7, showing the courses of tether length, reference length, and distance between the drones during the simulations. The chosen references are 0.5 m larger than the drones' distances, and they are tracked with good accuracy by the winch controllers.

6 Conclusions and future research

We proposed a modeling and control design framework for a new class of unmanned aerial vehicles, named systems of tethered multicopters (STEM), composed of a series of tethered multi-copter drones. Differently from previous works

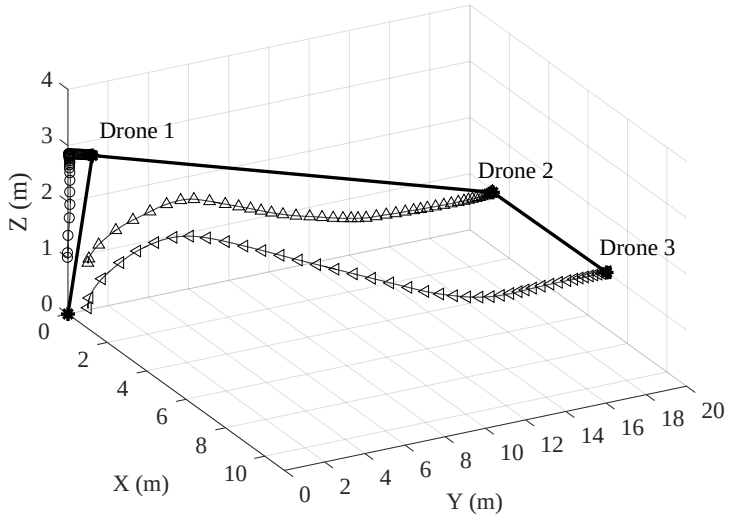

Figure 4: Simualtion results of a three-drone STEM. Trajectories of the three tethered drones in the inertial frame G.

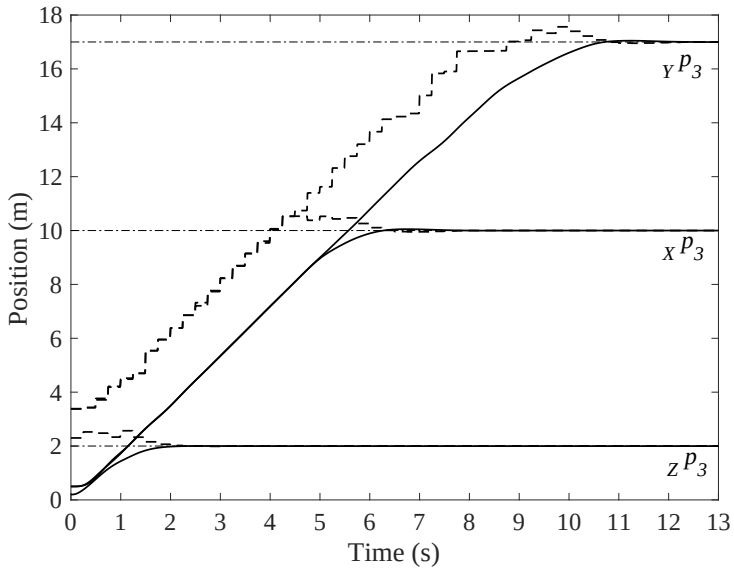

Figure 5: Simualtion results of a three-drone STEM. Courses of the (X, Y, Z) position components of drone $i = 3$ (solid lines), reference values issued by the MPC law (dashed), and desired target (dash-dot).

in the literature, flexible tethers in three-dimensional space are considered here. Moreover, the tethers' lengths can be adjusted by means of winches installed in the ground station and on the drones. The proposed control design approach is hierarchical, with local decoupled controllers on each drone and winch, and a

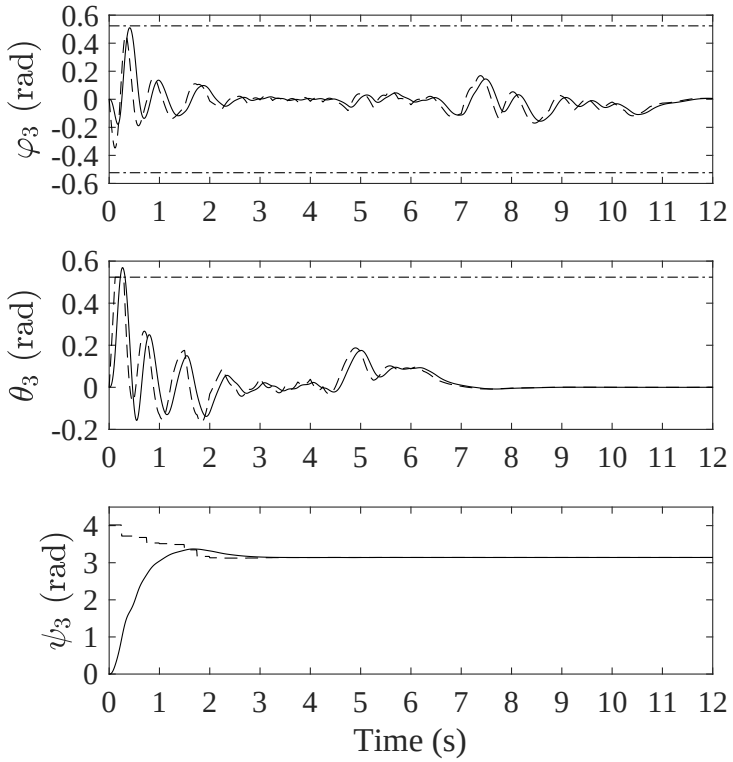

Figure 6: Simualtion results of a three-drone STEM. Trajectories of the roll, pitch and yaw angles of drone $i = 3$ (solid lines), reference values issued either by the velocity control loop (for φ_3 and θ_3) or by the MPC law (for ψ_3) (dashed lines).

supervisory model predictive control law to coordinate the whole formation, in order to pursue the considered control task and enforce the desired operational constraints.
The next steps of this research will be aimed at the construction and testing of a prototype STEM, and the investigation of a number of aspects including system design, modeling, filtering, control, and applications of the technology.

References

[1] Boyd, S. and Vandenberghe, L. (2009). *Convex Optimization*. Cambridge University Press, New York.

[2] Choi, S.Y., Choi, B.H., Jeong, S.Y., Gu, B.W., Yoo, S.J., and Rim, C.T. (2014). Tethered aerial robots using contactless power systems for extended mission time and range. In *IEEE Energy Conversion Congress and Exposition*, 912–916.

[3] Elistair (2016). Company website: http://elistair.com/, last accessed september 2016.

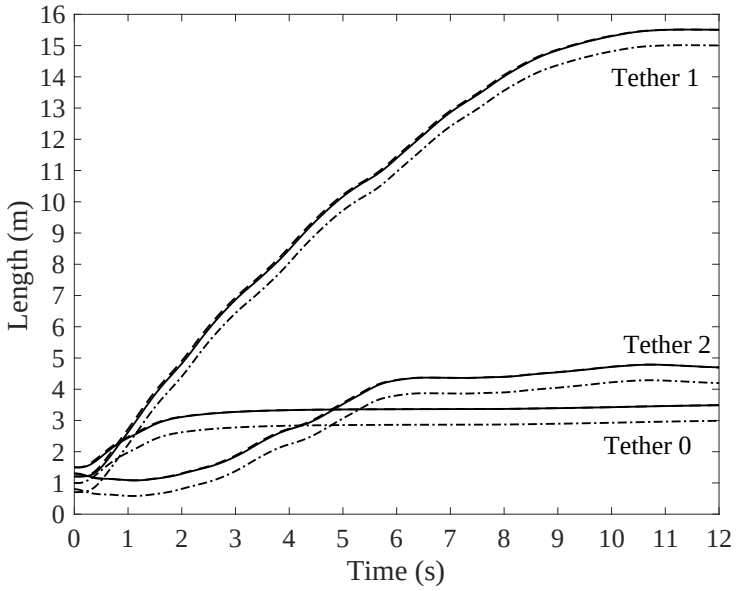

Figure 7: Simualtion results of a three-drone STEM. Courses of the reference tether length (dashed line), the actual one (solid), and the corresponding distances between the drones (dash-dot). The reference and actual tether lengths are computed from the reference and acutal winch angular position.

[4] Fagiano, L., Nguyen-Van, E., Rager, F., Schnez, S., and Ohler, C. (2016). Autonomous take off and flight of a tethered aircraft for airborne wind energy. *ArXiv e-prints: 1608.01889*, http://arxiv.org/abs/1608.01889.

[5] Formentin, S. and Lovera, M. (2011). Flatness-based control of a quadrotor helicopter via feedforward linearization. In *50th IEEE Conference on Decision and Control and European Control Conference (CDC-ECC)*, 6171–6176.

[6] Goodwin, G.C., Seron, M., and Dona, J.D. (2005). *Constrained Control and Estimation: An Optimisation Approach*. Springer.

[7] Goodwin, G.C., Graebe, S.F., and Salgado, M.E. (2001). *Control System Design*. Prentice-Hall, Upper Saddle River, NJ.

[8] Keemink, A., Fumagalli, M., Stramigioli, S., and Carloni, R. (2012). Mechanical design of a manipulation system for unmanned aerial vehicles. In *IEEE International Conference on Robotics and Automation (ICRA)*, 3147 – 3152.

[9] Lee, T. (2015). Geometric controls for a tethered quadrotor uav. In *IEEE Conference on Decision and Control*, 2749–2754. Osaka, Japan.

[10] Leonard, J., Savvaris, A., and Tsourdos, A. (2013). Energy management in swarm of unmanned aerial vehicles. In *International Conference on Unmanned Aircraft Systems (ICUAS)*, 124–133.

[11] Lupashin, S. and D'Andrea, R. (2013). Stabilization of a flying vehicle on a taut tether using inertial sensing. In *IEEE/RSJ Int. Conf. on Intelligent Robots and Systems*, 2432–2438.

[12] Naldi, R., Gasparri, A., and Garone, E. (2012). Cooperative pose stabilization of an aerial vehicle through physical interaction with a team of ground robots. In *IEEE Int. Conference on Control Applications*, 415–420.

[13] Nemra, A. and Aouf, N. (2010). Robust ins/gps sensor fusion for uav localization using sdre nonlinear filtering. *IEEE Sensors Journal*, 789–798. 4.

[14] Oh, S., Pathak, K., Agrawal, S.K., Pota, H.R., and Garrett, M. (2006). Approaches for a tether-guided landing of an autonomous helicopter. *IEEE Transactions on Robotics*, (22), 536–544.

[15] Tayebi, A. and McGilvray, S. (2006). Attitude stabilization of a vtol quadrotor aircraft. *IEEE Transactions on Control Systems Technology*, (14), 562–571.

[16] Tognon, M., Dash, S.S., and Franchi, A. (2016). Observer-based control of position and tension for an aerial robot tethered to a moving platform. *IEEE Robotics and Automation Letters*, 732–737.

[17] Tognon, M. and Franchi, A. (2015). Control of motion and internal stresses for a chain of two underactuated aerial robots. In *14th European Control Conference*, 1620–1625. Linz, Austria.

[18] Tognon, M. and Franchi, A. (2015). Nonlinear observer for the control of bi-tethered multi aerial robots. In *IEEE/RSJ Int. Conf. on Intelligent Robots and Systems*, 1852–1857.

[19] Valavanis, K.P. and Vachtsevanos, G.J. (eds.) (2014). *Handbook of Unmanned Aerial Vehicles*. Springer Netherlands.